Anomalous Thermal Behavior of Salicylsalicylic Acid and Evidence for a Monotropic Transition to a Nematic Phase

Joaquim J. Moura Ramos,*,† Hermínio P. Diogo,‡ Maria Helena Godinho,§ Carlos Cruz,# and Katarzyna Merkel⊥

Centro de Química-Física Molecular, Complexo I, IST, Av. Rovisco Pais, 1049-001 Lisboa, Portugal, Centro de Química Estrutural, Complexo I, IST, Av. Rovisco Pais, 1049-001 Lisboa, Portugal, Departamento de Ciência dos Materiais and CENIMAT, Faculdade de Ciências e Tecnologia, Universidade Nova de Lisboa, 2829-516 Caparica, Portugal, Centro de Física da Matéria Condensada, Av. Prof. Gama Pinto 2,1649-003 Lisboa e Departamento de Física, IST, Av. Rovisco Pais, 1049-001 Lisboa, Portugal, and Department of Electronic and Electrical Engineering, Trinity College, University of Dublin, Dublin 2, Ireland

Received: January 8, 2004; In Final Form: March 19, 2004

The temperature of maximum intensity of the isotropization peak of salicylsalicylic acid, obtained by differential scanning calorimetry (DSC), is reported to display a strong dependence on the heating rate. A detailed analysis of the DSC results combined with polarizing optical microscopy (POM) observations and X-ray diffraction (XRD) measurements, as a function of temperature, gives evidence for a nematic phase that appears when the sample is heated. In the present work, some experimental results are presented that suggest that the thermal behavior of the salicylsalicylic acid and the formation of the nematic phase are associated with a process that has slow kinetics. The molecular mobility in the crystalline phase of salicylsalicylic acid was studied by thermally stimulated depolarization currents.

1. Introduction

The melting of a crystal is often described as a first-order thermodynamic transition (P. Ehrenfest classification). This type of phase transition is accompanied by discontinuous changes of thermodynamic properties such as enthalpy and density, and these changes occur at a given, well-defined, temperature. It is sometimes noted that the melting temperature depends on the heating rate. However, this dependence is very slight in most cases, and it results not from the physical nature of the substance, but rather from the nonideality of the equipment, namely from some inefficiency in the heat transfer between the instrument and the sample. The melting of a crystalline polymer, on the other hand, shows some features that are different from the melting of molecular crystals. In fact, for polymers, it is not possible to define a unique melting temperature, given that the melting process occurs over a wide temperature interval, as a consequence of the molecular weight polydispersity.[1] On the other hand, the melting temperature of gels depends on the rate of gelation and, thus, on the thermal history of the material.[1] Furthermore, the formation of a liquid film at the surface of a crystal can occur at temperatures well below the melting temperature, and this occurs in polymers as well as in low-molecular-weight substances.[1] These premelting phenomena add some complexity to the melting process. Another factor that can introduce complexity in the solid−liquid phase transition is superheating. However, it is generally agreed that the superheating of a crystal is an infrequent occurrence (compared with the supercooling of a liquid), and that the temperature interval where it occurs is very narrow.[1]

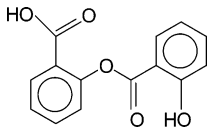

Figure 1. Chemical structure of salicylsalicylic acid. The internal rotation through 120° places the OH group (linked to aryl ring) adjacent to either the carboxylic or ester groups.

Salicylsalicylic acid (also called salicyl salicylate or salsalate) is reported to be a substance with a very peculiar thermal behavior, which can be attributed to the presence of intramolecular and intermolecular hydrogen bonding interactions.[2]

The structure of salsalate is shown on the Figure 1. The hydroxy group (OH) occupies the *ortho* position on an aryl ring, and the internal rotation through 120° places this group adjacent to either the carboxylic or ester groups. Both configurations maybe influenced by formation of intramolecular hydrogen bonds. The two possible configurations of the salsalate can be the result of two intramolecular hydrogen bonding networks in this drug crystal.[1,3] This compound can also form an intermolecular hydrogen bond, which is very important when the referenced unusual behavior is studied.

Finally, salicylsalicylic acid presents an enormous resistance to crystallization.[2] In fact, cooling the melt has been observed to lead to a high-viscosity supercooled liquid that can be molded and stress-fractured without crystallizing. Furthermore, it was observed that crystallization in salicyl salicylate could not be induced by any means, including crystal seeding, and that recrystallization could be achieved only by dissolution and reprecipitation.[2]

On the other hand, a pronounced differential scanning calorimetry (DSC) peak is most evident over the range of 139−

* Author to whom correspondence should be addressed. Telephone: 351-21-8419253. Fax: 351-21-8464457. E-mail address: mouraramos@ist.utl.pt.
† Centro de Química-Física Molecular, Complexo I.
‡ Centro de Química Estrutural, Complexo I.
§ Universidade Nova de Lisboa.
# Centro de Física da Matéria Condensada.
⊥ University of Dublin.

10.1021/jp049903v CCC: $27.50
Published on Web 05/07/2004

151 °C (412−424 K, for a heating rate of 10 K/min), and its location seems to be strongly dependent on the heating rate. This particular behavior led us to perform a study of salicyl salicylate using DSC, to elucidate its thermal behavior. In a previous work,[4] we studied the glass transition in detail. In the present work, we present some results to clarify the thermal behavior near the melting point. The existence of an additional peak at 118−120 °C (for an heating rate of 20 K/min) in the DSC profile and a "shoulder" preceding the isotropization peak suggest the existence of at least one mesophase that appears when the temperature is increased from the crystal to the isotropic phase. Polarizing optical microscopy (POM) observations and X-ray diffraction (XRD) results, obtained as function of temperature, confirmed the formation of a particular nematic phase. The structure of this mesophase and the peculiar slow kinetics associated with its formation were investigated through the combination of the DSC results with POM and XRD studies as a function of time at the crystal−mesophase transition temperature.

2. Experimental Section

Salicyl salicylic acid (CAS number 552-94-3) supplied by Acros (mass fraction of >0.99), was used after recrystalization from water. Fifty grams of the sample was dissolved in boiling distilled and deionized water, filtered into a thermostated double-wall beaker, and then cooled to 275 K at a rate of ca. 1.4×10^{-3} K/s, by circulating water from a Julabo model F25-EC temperature controller. The precipitated salicyl salicylate was removed from the mother liqueur by vacuum filtration and dried in an oven for 3 h at a temperature of 363 K. Elemental analysis that was conducted using a Fisons Instruments model EA1108 apparatus led to the following results for the mass fractions of carbon and hydrogen in $C_{14}H_{10}O_5$: Calcd.: C, 0.6512; H, 0.0390; found: C, 0.6509; H, 0.0392 (average of two independent runs). The Fourier transform infrared (FTIR) spectrum of the sample in KBr determined with a Jasco model 430 spectrophotometer calibrated with polystyrene film is similar to one published in the literature and does not reveal the band attributed to water absorption.[5] The ^{1}H NMR spectra performed in $CDCl_3$, at room temperature, on a Varian 300 MHz spectrometer was as follows (chemical shifts, δ, relative to tetramethylsilane): $\delta/10^{-6} = 10.24$ (s, COOH, 1H), 8.12 (dd, CH, 1H), 8.05 (dd, CH, 1H), 7.66 (m, CH, 1H), 7.51 (m, CH, 1H), 7.39 (m, CH, 1H), 7.25 (m, CH, 1H), 6.99 (m, CH, 1H), 6.92 (m, CH, 1H), which are in good agreement with the spectra reported in the literature.[2] Powder X-ray diffractometry (XRD) was performed with a Rigaku Geigerflex diffractometer, using Cu Kα radiation, over the range of $5° \leq 2\theta \leq 35°$. The powder patterns were indexed as monoclinic, using the Chekcell program.[6] The space group was identified as *Cc*, with $a =$ 1307.9(9) pm, $b =$ 1296.4(8) pm, $c =$ 1554.2(6) pm, and $\beta =$ 113.81°. These values are in excellent agreement with those obtained by single-crystal XRD experiments ($a =$ 1296.5(4) pm, $b =$ 1298.2(4) pm, $c =$ 1553.0(3) pm, and $\beta =$ 114.039°).[2] The indexation of the lines was presented in a previous work.[4]

Temperature-dependent XRD measurements on powder samples were performed using a variable-geometry device equipped with a Max-Flux Optic graded multilayer monochromator (Cu Kα radiation) and a gas curved counter "INEL CPS 590" that was associated with a data acquisition computer-controlled system. This device is equipped with a computer-controlled electric oven. The temperature of the sample was controlled within ±0.1 °C. The measurements were performed in the range from 25 °C to 160 °C with a step of 1 °C.

The optical observations were performed on thin samples pressed between two glass slides. Textures were observed and optical microphotographs were taken, as a function of temperature, with an Olympus polarizing light microscope that was equipped with a Mettler model FP52 hot stage and a camera. Photos were taken after salsalate recrystallization from diethyl ether at room temperature.

The DSC measurements were performed with a model 2920 MDSC system from TA Instruments, Inc. Dry, high-purity helium gas (ArLiquide, N55) at a flow rate of 30 cm^3/min was purged through the sample, which was previously encapsulated in an aluminum pan and weighed ($\pm 10^{-7}$ g) with a Sartorius 4504 Mp8-1 ultramicrobalance. Cooling was accomplished with the liquid nitrogen cooling accessory (LNCA), which provides automatic and continuous programmed sample cooling to −150 °C. The details relative to the calibration procedures were given elsewhere.[4,7]

Thermally stimulated depolarization current (TSDC) experiments were performed using a model TSC/RMA 9000 spectrometer (TherMold Partners, Stamford, CT) covering the temperature range between −170 °C and +400 °C. Several references explaining the physical background of TSDC are available[8−10] that can be useful for readers not familiar with this experimental technique. Moreover, several recently published papers[11,12] can be helpful to explain the experimental procedures used in TSDC and the physical meaning of the data provided by this technique.

3. Results and Discussion

Figure 2 shows the thermogram of salicylsalicylic acid obtained via DSC at different linear heating rates, from room temperature up to 180 °C.

From the analysis of these results, we concluded that the enthalpy associated with the clearing point is $\Delta_m H = 112$ J/g (= 29.0 kJ/mol^{-1}). The melting enthalpy was calculated by integrating the area of the endothermic peak using a sigmoidal baseline. The same value was obtained from the different experiments with different heating rates. Figure 2 shows that the onset temperature of isotropization seems to be the same, or at least almost independent of the heating rate ($T_{on} =$ 143−147 °C), whereas the temperature of maximum intensity of the clearing peak (T_{max}) appreciably increases as the heating rate increases. The shape of the peaks obtained at different heating rates is such that the lower-temperature side seems to be approximately similar to all the peaks. The increase of the temperature of maximum intensity of the melting peak (T_{max}) with increasing heating rate is a general observation, even for substances that are used as standards to calibrate the temperature scale of DSC calorimeters (indium and benzoic acid, for example). However, we found the shift of the peak position for different heating rates for these standard materials to be very short (not exceeding 1 or 2 K, for heating rates of 0.5−20 K/min). In contrast, in the case of salicylsalicylic acid, a marked shift to higher temperatures is observed, extending to >20 K, which appears as rather unusual behavior.

A possible origin for the observed behavior could be the existence, in the phase diagram of salicylsalicylic acid, of an intermediate phase in a short temperature domain between the crystal and the isotropic liquid. In fact, a more detailed observation of the thermograms reveals (besides the pronounced peak ($\Delta H =$ 29.0 kJ/mol) detected at 157 °C (heating rate of 20 °C/min) corresponding to the transition to the isotropic phase), the existence of a smaller peak at a temperature of 118 °C also is characteristic of a first-order phase transition, with

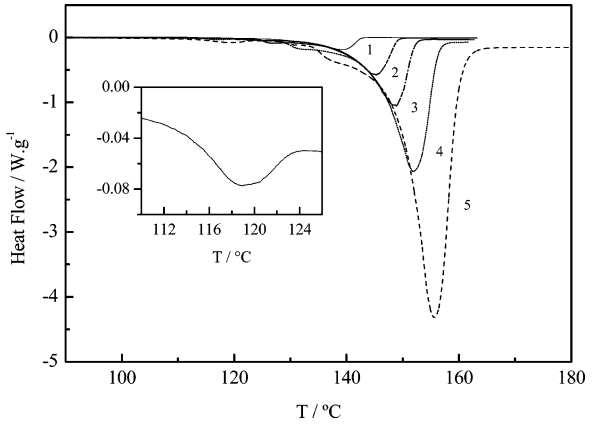

Figure 2. Endothermic melting peak of salicylsalicylic acid obtained at different linear heating rates. Curves 1−5 respectively correspond to heating rates of 1, 3, 5, 10, and 20 K/min. Given that the compound does not recrystallize, the different curves in this figure correspond to different samples. Inset shows an enlarged view of the curve obtained at 20 K/min at ∼118 °C.

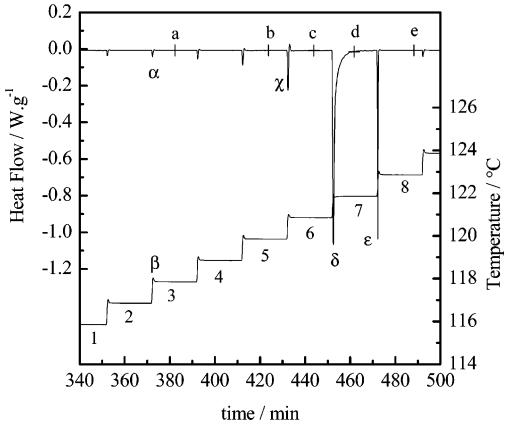

Figure 3. Melting of benzoic acid obtained in a DSC experiment where the heating process is performed in successive isothermal steps. The top curve shows the experimental result of the experiment (heat flux, as a function of time), whereas the lower line schematically displays the experimental procedure (temperature as a function of time). The temperature at step 1 is 115.9 °C (389.1 K), the temperature jumps are $\Delta T = 1$ K, and the duration of the isothermal steps is $\Delta t = 20$ min. Heat flow values at the marked points are as follows: −0.0077 W/g (a), −0.0078 W/g (b), −0.0087 W/g (c), −0.0146 W/g (d), and −0.0077 W/g (e).

an enthalpy of $\Delta H < 0.25$ kJ/mol. As will be reported later, this temperature corresponds to an important change in the XRD profile that occurs at this temperature. It is important to note that the DSC curves obtained on cooling from the isotropic liquid do not show any crystallization signal. Furthermore, no singularity was observed at ∼118 °C in these DSC results obtained on cooling. This irreversible character of the phase transitions is discussed in Section 3.3.

To investigate the existence of a mesophase we subjected a crystalline sample to POM observations and XRD measurements. Both optical and XRD experiments were performed specifically at the temperature range where the mesophase hypothetically exists. Measurements as a function of time (both POM and XRD) were conducted to better understand the unusual thermal behavior of the sample as observed by DSC. These detailed measurements would not only serve to confirm the existence of the intermediate phase but also to characterize its molecular organization.

3.1. Detailed Study of Thermal Behavior by Differential Scanning Calorimetry. To gain some more insight on the origin of the observed thermal behavior, we subjected the sample to an experimental protocol that causes the temperature to increase a specified number of degrees in a specified time interval until a final temperature, above the clearing temperature, is reached. The experimental procedure is thus a heating process composed by successive isothermal steps: the temperature changes not as a linear ramp but rather in a stepwise manner. The experimental procedure previously described was applied to a sample of salicylsalicylic acid and also, for comparison, to a sample of standard benzoic acid.

3.1.1. The Melting Behavior of Benzoic Acid. Figure 3 shows the results obtained with benzoic acid. Before we discuss the analysis of the results relative to the melting process, we will comment on some general features of Figure 3 that result from the particular procedure used in the present experiment. First note that, to increase the temperature between two successive steps, a given quantity of heat must be supplied to the sample. This results in a small endothermic peak in the heat flow (for example, α in Figure 3). Moreover, we can observe a small temperature overshoot at the end of each transition between adjacent steps (for example, β in Figure 3). Note also that, far from the melting temperature region, the heat flow in the different isothermal steps is almost the same (approximately −0.0077 W/g in steps 1, 2, 3, and 4 in Figure 3).

In the experimental result relative to the melting temperature region of benzoic acid, reported in Figure 3, one can identify two manifestations of the melting process: (i) isothermal melting, which occurs in each step of the stairs; and (ii) melting on heating, which occurs in the heating process that leads from one step to the next. This melting process that occurs between two successive steps appears as an endothermic spike (χ, δ, and ϵ in Figure 3), given that the heating rate leads to an amplification of the thermal effects ($\dot{Q} = C_P\dot{T}$). Let us observe what happens when the melting temperature region of benzoic acid is approached. The fact that the intensity of the endothermic peak χ between steps 5 and 6 is higher than that of the peaks at lower temperatures (from step 1 to step 5) indicates the beginning of the melting process, as the sample is heated from 119.9 °C to 120.9 °C. In isothermal step 6, at 120.9 °C, the heat flow that enters the sample is slightly higher than that in the previous steps (approximately −0.0088 W/g, instead of −0.0077 W/g), indicating a slow and constant rate melting during this step. The strong endothermic peak δ in the heat flow between steps 6 and 7 (as the sample is heated from 120.9 °C to 121.9 °C) corresponds to the melting of most of the sample. The temperature overshoot is absent between steps 6 and 7, given that it was canceled by the high amount of heat absorbed by the sample. Note also that the melting process extends through isothermal step 7, in such a way that the heat flow decreases as the time increases. The fraction of the sample not melted at the end of isothermal step 7 melts in the heating ramp between steps 7 and 8 (endothermic peak ϵ), and the heat flow recovers the value of −0.0077 W/g in step 8 and the subsequent steps. From Figure 3, we can conclude that benzoic acid melts in a narrow temperature range—between 119.9 °C and 122.9 °C—and that the melting rate is higher at 121.9 °C.

3.1.2. The Thermal Behavior of Salicylsalicylic Acid near the Clearing Temperature. Salicylsalicylic acid was subjected to the same experimental protocol as that shown in Figure 3 for benzoic acid. The results are presented in Figure 4.

The first general conclusion that we can draw from the comparison of Figures 3 and 4 is that the thermal behavior of salicylsalicylic acid is strikingly different from that observed for benzoic acid. We can conclude from Figure 4 that the DSC

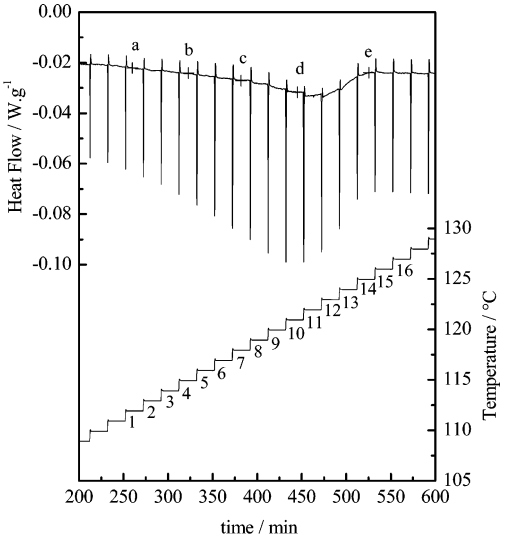

Figure 4. Melting of salicylsalicylic acid obtained in a DSC experiment where the heating process is performed in successive isothermal steps. The top curve shows the experimental result of the experiment (heat flux as a function of time), whereas the lower line schematically displays the experimental procedure (temperature as a function of time). The temperature at step 1 is 111.9 °C (385.1 K), the temperature jumps are $\Delta T = 1$ K, and the duration of the isothermal steps is $\Delta t = 20$ min. Heat flow values at the marked points are as follows: −0.0220 W/g (a), −0.0241 W/g (b), −0.0271 W/g (c), −0.0317 W/g (d), and −0.0240 W/g (e).

signal in salicylsalicylic acid is very broad in the temperature axis, extending from ∼115 °C (step 4) up to 126 °C (step 14). There is a slow endothermic evolution from step to step. From the values of the heat flow in each step, we can conclude that the clearing rate (quantity of sample changing to isotropic phase per unit time) increases until 122 °C (step 11) and then decreases subsequently with increasing temperature, so that, at 127 °C (step 15), the sample is fully isotropic.

To explain the thermal behavior of salicylsalicylic acid on melting, the hypothesis of superheating could be considered. In this context, the idea is to consider that increasing the heating rate would increase the depth of the plunge in the metastable temperature region (the degree of superheating), leading to an increase of the melting temperature. The result previously reported seems to rule out the hypothesis of metastability of the crystal as an explanation of the melting behavior of salicylsalicylic acid. However, in an experiment such as that presented in Figure 4, the 20-min isothermal steps would prevent a deep penetration in the solid metastability region, leading to a sharp melting temperature region, similar to that of benzoic acid, which is not observed. Oppositely, the obtained result clearly shows that the isotropization process in salicylsalicylic acid is broad and proceeds progressively with slow kinetics as the temperature increases. As noted previously, it is generally agreed that (i) the superheating of a crystal is difficult to observe (compared, for example, to the supercooling of a liquid) and (ii) it occurs in very narrow temperature intervals. Accordingly, the conclusion that the superheating of the crystal is probably not the source of the observed behavior is not unexpected.

An alternative explanation turns to the idea of a depression of the melting temperature. Two aspects should be considered. The first is the enlargement of the melting peak, and the second is the apparent kinetic behavior of the melting process. The enlargement of the peak may result from the effect of the size distribution of the crystals, or from the effect of crystal defects (holes, displacements, etc.). The presence of small crystallites,

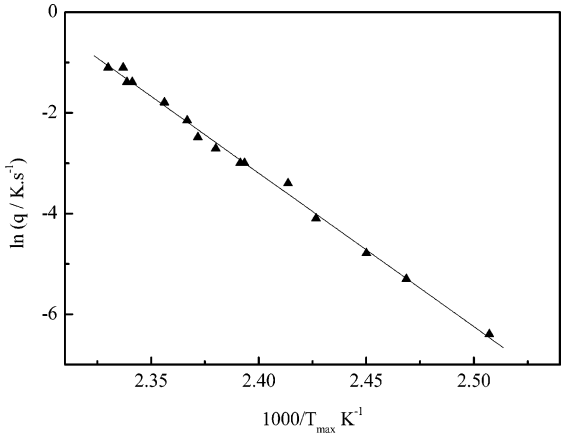

Figure 5. Heating rate dependence of the temperature of maximum intensity (T_{max}) of the melting peak of salicylsalicylic acid, represented as the logarithm of heating rate, q, as a function of T_{max}.

as well as a high defect concentration, produces a depression of the melting temperature. This will depend on the mode of preparation of the crystalline sample. A population of highly defective crystallites could explain the width of the melting peak but not the effect of the heating rate (kinetic behavior). Oppositely, the effect of the particle size (Gibbs−Thomson effect) could explain the observed behavior, but the presence of nanoscopic particles is necessary to cause a sensible depression of the melting temperature. To understand the influence of the particle size on the melting behavior of salicylsalicylic acid, we prepared samples with different particle size distributions, making use of two calibrated sieves. The crystalline material was sifted through a sieve of 0.063 mm (230 mesh), and the crystals that passed through that sieve were sifted through a sieve of 0.038 mm (400 mesh). We thus prepared three samples with different particle size distributions: one with large particles (with dimensions of >0.063 mm), where nanocrystals are absent; another one with particles whose dimensions are 0.063−0.028 mm, where nanocrystals are also absent; and the third one with smaller particles (with dimensions of <0.028 mm), where nanocrystals are eventually present. The DSC melting peak was obtained for these different samples at different heating rates, and the obtained results showed that the effect of the heating rate on the melting temperature (T_m) is the same for the three samples. Moreover, for the same heating rate, the particle size does not affect the position of the melting peak significantly.

Let us finally note that the enlargement of the melting peak can also be due to a progressive disruption of the hydrogen bonding network. As will be shown later from the POM observation and from the X-ray analysis, the thermal behavior may be associated with the progressive transformation of the crystal domains into nematic ones, ran by the hydrogen bonding network rearrangement.

3.1.3. Heating Rate Dependence of the Melting Peak Location. The heating rate dependence of the temperature of maximum intensity (T_{max}) is illustrated in Figure 5 which shows the representation of the logarithm of heating rate as a function of the reciprocal of the T_{max} value of the melting peak of salicylsalicylic acid.

The fact that the representation is almost linear (correlation coefficient of $r = 0.998$) suggests that the shift of the melting peak position probably has a kinetic origin. If we assume an energy barrier at the origin of the observed behavior, the corresponding activated energy obtained from the slope of the representation is 250 kJ/mol.

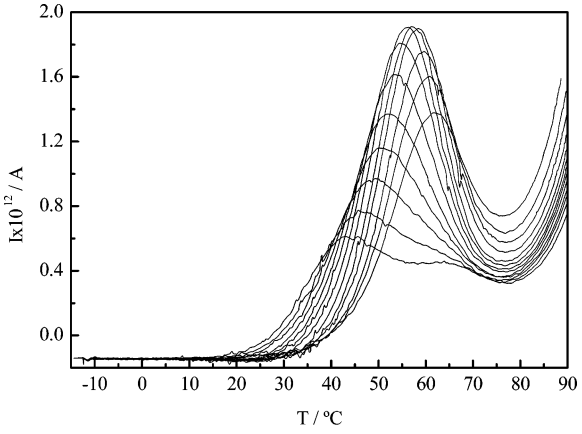

Figure 6. Thermally activated components of the relaxation observed by TSDC in the crystalline phase of salicylsalicylic acid. Polarization temperatures used in the experiments were from $T_p = 36-60$ °C, at intervals of 2 °C. The other experimental conditions were as follows: polarization time, $t_p = 5$ min; width of the polarization window, $\Delta T = 2$ °C; strength of the polarization field, $E = 450$ V/mm; and heating rate, $q = 4$ °C/min.

To get a better understanding of the phenomenon, we performed a study of the molecular mobility in the crystalline salicylsalicylic acid, using the technique of thermally stimulated currents.[13] Figure 6 shows the results of some TSDC experiments performed in the crystalline phase. The peaks shown correspond to a mobility mode in the crystal that becomes free at a temperature above ~60 °C. It is a mode of motion characterized by a barrier of 150 kJ/mol, and by an activation entropy of 170 J K^{-1} mol^{-1}.

We can speculate that the existence of a slow thermally activated mobility mode, near the melting temperature, could be a prerequisite for melting and could give a kinetic character to the melting process. However, the mode of motion observed at ~60 °C is probably too far from the melting temperature to cause this effect. Furthermore, the activation energy of this mobility mode (150 kJ/mol) seems to be low, compared to the barrier that would be needed to cause the observed shift of the melting peak position (250 kJ/mol). Unfortunately, the presence of a conductivity tail for temperatures higher than ~100 °C did not allow the analysis of the mobility in the vicinity of the melting temperature.

3.2. Polarizing Optical Microscopy Studies. As mentioned previously, the DSC trace obtained at a rate of 20 °C/min on heating from the crystalline phase shows a profile with a small peak at ~118 °C and another at 155 °C. To understand the behavior detected by DSC, optical measurements were performed. As usual for liquid crystalline phases, when the temperature increases, we only observe clearly some small modifications in the optical textures at the phase transition between crystalline phase and the mesophase. Generally, the characteristic textures of mesophases are clearly developed by decreasing the temperature from the isotropic phase. However, the transition from isotropic to mesophase or crystal phase is not reversible for salsalate.

The crystalline film for observation in the optical microscope was prepared from a drop of a solution of salsalate in diethyl ether that directly precipitates on the microscope slide glass. After preparing the sample, at room temperature (the crystalline texture observed is shown in Figure 7a), two types of procedures were performed. In the first one, the temperature was increased from 26 °C at a rate of 20 °C/min (the same rate used in DSC

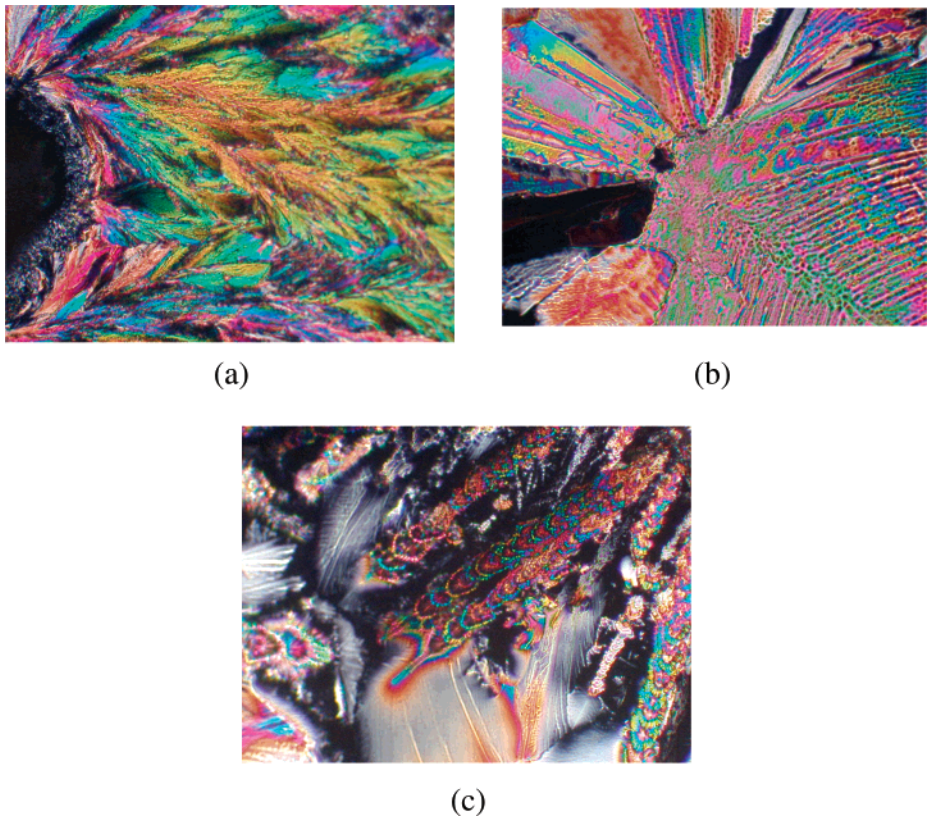

Figure 7. Textures of salicylsalicylic acid observed with cross polarizers: (a) crystalline texture at room temperature, after recrystallization in diethyl ether; (b) textures observed in the nematic phase at 119 °C, after a waiting time of 30 min; and (c) textures observed in the nematic phase at 119 °C, after a waiting time of 50 min. The magnification factor of the camera was 250×.

experiments) and no significant texture modification that was associated with the first phase transition detected by DSC was observed.

In a second test, the sample temperature was changed directly from $T = 26$ °C to $T = 119$ °C and maintained constant for several minutes. It was then possible to observe a modification of the crystalline texture with time. After 20 min, a new texture that contains domains of uniform birefringence starts to develop (see Figure 7b), and after 50 min, some isotropic regions start to coexist with large areas of birefringent material and spirals (Figure 7c). The domains observed are not characteristic of a nematic schlieren or marbled texture[14] but are quite different from the crystalline phase. By shearing the sample, larger birefringent areas develop. This type of texture can be preserved on cooling to room temperature. As will be discussed in Section 3.3, the textures observed and the liquid flow properties of the material can be associated with a nematic mesophase as detected by X-ray measurements.

3.3. X-ray Diffraction Measurements and Phase Structure Discussion. To clarify the nature of the mesophase observed by POM, powder XRD patterns were registered in the temperature range of 25−160 °C with a step of 1 °C. Waiting times of 10 or 30 min were respected before the data acquisition at each temperature below and above 112 °C, respectively. The acquisition time at each temperature was 1 h. Time-dependent measurements were also conducted at 118, 118.5, 119, and 119.5 °C to check for possible observations of phase-transition kinetics effects. Our results in the range of temperatures within the crystal phase were compared with previous data[3] obtained at room temperature, to which they are similar, as expected. At 118 °C, we found a significant change in the XRD profile (see Figure 8a). The Bragg peaks that are characteristic of the crystal phase disappear and are replaced by a pattern formed by broad peaks that are characteristic of a disordered phase. This is in agreement with the results from DSC and POM. The observed modification of the XRD pattern is typical of a transition from a crystalline phase to an isotropic liquid or to a nematic liquid crystal.

The birefringence of the sample as shown by POM in the range of 118−151 °C excludes the existence of an isotropic phase, which would be immediately identified by the light extinction in the optical observation between cross polarizers.

On the other hand, the total absence of Bragg peaks in the XRD patterns excludes the possibility of long-range positional order, which means that the observed mesophase does not exhibit any type of lamellar or columnar symmetry. The birefringence observed should be due to some type of molecular collective orientation without long-range positional order. From the combination of POM and XRD observations, we may therefore conclude that the observed mesophase is a nematic one.

Our X-ray data show three broad peaks, corresponding to three main characteristic distances. The values of these distances were determinate by fitting of Gaussian functions to the XRD pattern as shown in Figure 9. The average values of these distances, deduced from the X-ray patterns, are 3.8, 5.3, and 8.6 Å. Two of these distances (3.8 and 5.3 Å) can be straightforwardly assigned to short-range positional order of the aromatic rings, with 5.3 Å being the lateral distance between the centers of two aromatic rings placed side by side and 3.8 Å being the distance between the planes corresponding to the stacking of two aromatic rings on top of each other. Similar distances appear currently in the packing of liquid crystals of calamitic[15] and discotic[16] molecules, respectively. The third

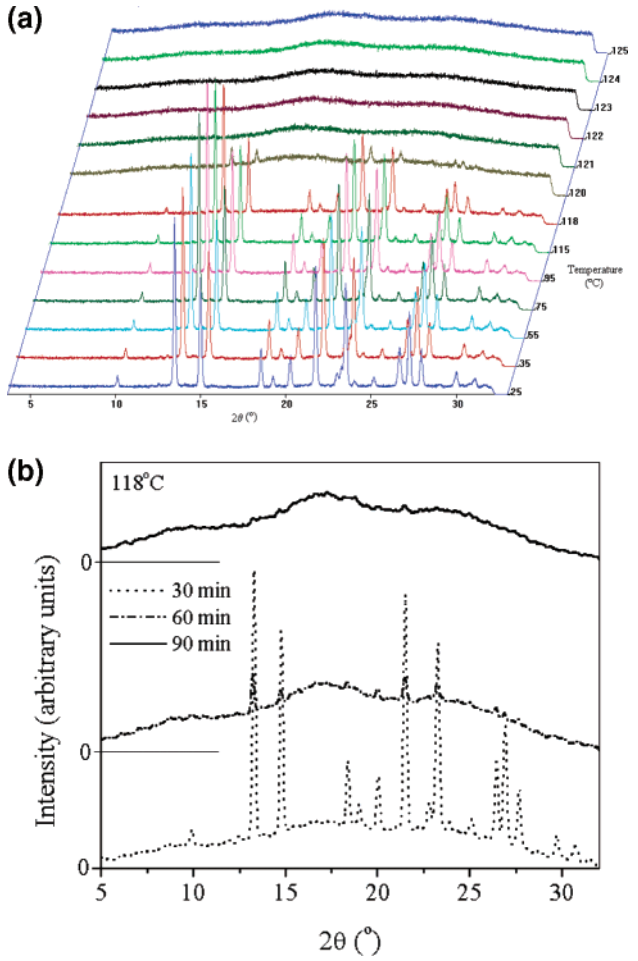

Figure 8. Powder X-ray diffraction (XRD) profiles (a) as a function of temperature (vertical scale given in arbitrary units) and (b) time for $T = 118$ °C.

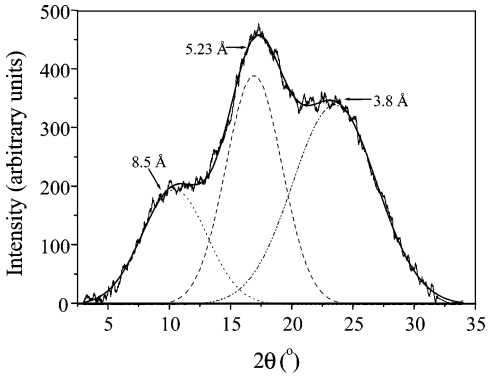

Figure 9. Fit of Gaussian functions to the XRD profile at 119 °C. The mean values of these functions respectively correspond to distances of 8.5, 5.3, and 3.8 Å.

distance (8.6 Å), and the way how the molecules are packed to ensure the short-range order of the aromatic rings responsible for the 3.8 and 5.3 Å peaks, needs to be explained.

At this point, the comparison of the XRD patterns of the salsalate mesophase and those of typical nematic phases of calamitic and discotic liquid crystals is useful. In those mesophases two peaks characterize the corresponding powder XRD pattern. These peaks are associated with the average dimensions of an ideal shape corresponding to the packing of the molecules: the length and diameter of a rod, in the case of calamitics, and the thickness and diameter of a disk, in the case of discotics. A value of ∼5 Å is normally found for the average

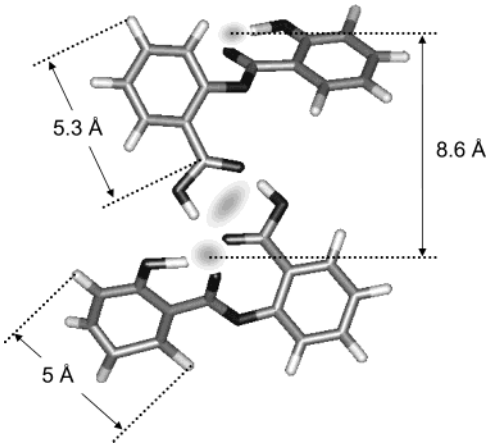

Figure 10. Z-shaped dimmer formed by salsalate molecules by intermolecular hydrogen bonding. The characteristic distance of 8.6 Å indicated in the figure corresponds to the separation of regions of intramolecular hydrogen bonds with high electronic density.

lateral distance between two rodlike molecules and a value of ~3.6 Å is found for the average thickness of a disklike molecule based, for instance, on a flat triphenylene core.[17] Additional values of the order of the tenths of angstroms characterize the length of the core or the diameter of the disk. According to our data, the mesophase exhibited by the salsalate is therefore peculiar. On one hand, a single molecule of the compound does not show either the pronounced anisometry that is characteristic of liquid crystalline compounds or the half-rigid, half-flexible structure normally exhibited by the mesogenic molecules. On the other hand, the distance corresponding to the third peak (8.6 Å) could not be attributed to any dimension related to the single molecule. However, if we consider intermolecular hydrogen bonding between two molecules, we will end up with an approximately flat Z-shaped dimmer with a considerable anisometry. Moreover, a characteristic dimension of this dimmer (see Figure 10) corresponds to the 8.6 Å distance determined by XRD.[2] Molecular simulations based on ab initio and semiempirical methods, considering intermolecular and intramolecular hydrogen bonding, are compatible with the formation of these quasi-flat dimmers.[18]

Finally, if we assume a discotic-like arrangement of these units, as shown in Figure 11, considering that Z-shaped dimmers can be packed by partially fitting them into each other, we verify that (i) the three average distances corresponding to the short-range electronic density periodicities observed by X-rays are present, and (ii) the anisotropy of the phase, which is responsible for the birefringence of the material, is due to the nematic discotic-like arrangement of the quasi-flat dimmers.

Actually, in the proposed model, the local packing of the Z-shaped dimmers allows for an uniform random distribution of the centers of the aromatic rings in the plane of the dimmers, leading to the broad peak corresponding to the 5.3 Å in the diffraction pattern. It is important to stress that the proposed molecular distribution does not imply any layer formation; instead, it suggests only a collective orientation of the average planes corresponding to the dimmers, in domains much larger than the molecular dimensions, such as those in a discotic nematic phase.[17] It is this collective orientation that leads to the observed birefringence. This type of packing also implies that, in the nematic domains, the neighboring molecules in the direction perpendicular to the dimmer average planes stay at an average distance that corresponds to the thickness of a benzene ring (3.6 Å), as normally observed in mesophases of discotic molecules. That explains the 3.6 Å peak. Finally,

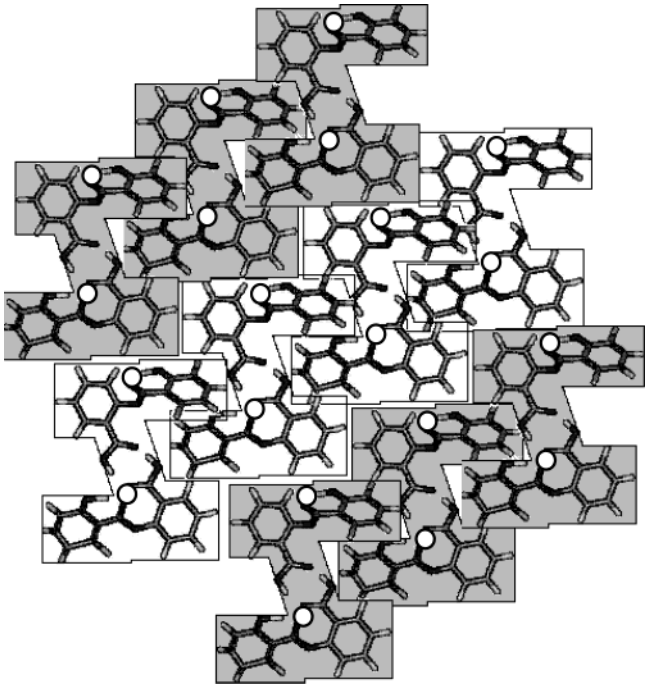

Figure 11. Top view of schematic local arrangement proposed for the Z-shaped dimmers. The circles corresponding to the high electronic density regions (associated with the intramolecular hydrogen bonds) are randomly distributed with a characteristic distance of ≅8.6 Å, according to XRD data.

considering that the dimmers have a longitudinal characteristic dimension of 8.6 Å, as shown in Figure 10, we can expect that a short-range periodicity exists in the electronic density results, as revealed by the corresponding peak in XRD pattern.

The observation of the evolution of the XRD patterns with time, at the crystal−mesophase transition temperature, is also significant. As we can see in Figure 8b, the slow formation of the mesophase is evidenced by the progressive disappearance of the Bragg peaks initially observed, leading to the broad peaks pattern, characteristic of the nematic phase. This process is extremely slow. As shown in Figure 8b, after 1 h, the phase transition is still not complete. Again, this observation agrees with the DSC results and the slow kinetics of the phase transition may be associated with the progressive transformation of the crystal domains to nematic ones (as observed by POM) ran by the hydrogen bonding network rearrangement from the crystalline lattice into a collection of orientationally ordered dimmers. The intermolecular hydrogen bonding, coupled with the rigidity that is due to the aromatic groups, influences the ordering, inducing liquid crystallinity and enhancing the phase stability. Note that the association and dissociation of the dimmers formed by intermolecular hydrogen bonding will contribute to the fluid character of the mesophase.

The irreversible character of the phase transitions can be associated with the asymmetry between the heating and cooling processes, in respect to the formation of the dimmers. At the crystal−mesophase transition, the probability of finding two molecules in positions adequate for the formation of a dimmer is high, leading to the formation of the nematic phase. When the sample reaches the isotropic phase, the structure formed by the dimmers is disrupted and the orientation of the molecules becomes randomly distributed. On cooling, the mobility of the molecules is most probably insufficient to ensure the highly directional arrangement necessary for the reconstitution of the dimmers, preventing the formation of the mesophase.

4. Conclusions

In this work, it was reported an anomalously strong heating rate dependence of the temperature of maximum intensity (T_{max}) of the differential scanning calorimetry (DSC) clearing peak of salicylsalicylic acid that is associated to the existence of a nematic phase between the crystal and the isotropic phase.

The melting behavior of salicylsalicylic acid was compared with that of benzoic acid, using an experimental procedure where the sample is heated in successive steps. The experimental results clearly showed strikingly different behavior for these two substances. It was observed that the melting process of benzoic acid is fast and occurs in a narrow temperature region, whereas that of salicylsalicylic acid is slow and extends over a wide temperature interval. It was concluded that the thermal behavior of salicylsalicylic acid does not result from superheating phenomena, but rather from the slow process that is associated with the formation of a nematic phase between the crystal and the isotropic phase.

The molecular mobility in crystalline salicylsalicylic acid was studied using thermally stimulated currents. A molecular relaxation was identified at ~60 °C; however, there is no evidence that this mobility is related to the observed melting behavior. The existence in the sample of a significant electrical conductivity above ~100 °C did not allow the analysis of the mobility in the vicinity of the melting temperature.

All the results obtained from DSC, polarizing optical microscopy (POM), and X-ray diffractometry (XRD) agree in the sense of the existence of a nematic phase that appears with increasing temperature between 118 °C and 157 °C. The structure of this nematic phase can be explained by the formation of dimmers through intermolecular hydrogen bonding. These dimmers, which work as mesogenic units, are packed similarly to the discotic molecules in a discotic nematic phase. The slow kinetics associated with the phase transitions on increasing temperature can be attributed to the importance of the hydrogen bonding interactions for the existence of the nematic phase. The irreversible character of the phase transitions observed may be associated with the highly steric selectivity imposed for the dimmer formation and the corresponding asymmetry between the heating and cooling processes.

Acknowledgment. We acknowledge Dr. Natália Correia for the help in the preparation of this manuscript.

References and Notes

(1) Papon, P.; Leblond, J.; Meijer, P. H. E. *Physique des Transitions de Phases: Concepts et Applications*; Dunod: Paris, 1999.

(2) Greener, B.; Archibal, S. J.; Hodkinson, M. *Angew. Chem., Int. Ed.* **2000**, *39*, 3601−3604.

(3) Cox, P. J.; Gilmour, G. I.; MacManus, S. M. *Int. J. Pharm.* **2000**, *204*, 133−136.

(4) Diogo, H. P.; Pinto, S. S.; Moura Ramos, J. J. Thermodynamic and Kinetic Behaviour of Salicylsalicylic Acid: A Calorimetric Study. *J. Therm. Anal. Calorim.*, in press.

(5) See Japanese web database: http://www.aist.go.jp.

(6) Laugier, J.; Bochu, B. Chekcell. (Available via the Internet at http://www.ccp14.ac.uk/tutorial/lmgp.)

(7) Moura Ramos, J. J.; Taveira-Marques, R.; Diogo, H. P. Estimation of the Fragility Index of Indomethacin by DSC Using the Heating and Cooling Rate Dependency of the Glass Transition. *J. Pharm. Sci.* **2004**, *93* (6), 1503−1507.

(8) Chen, R.; Kirsch, Y. *Analysis of Thermally Stimulated Processes*; Pergamon Press: Oxford, 1981.

(9) van Turnhout, J. *Thermally Stimulated Discharge of Polymer Electrets: A Study on Nonisothermal Dielectric Relaxation Phenomena*; Elsevier Science Publishing: Amsterdam, 1975.

(10) Teyssèdre, G.; Lacabanne, C. Some Considerations about the Analysis of Thermostimulated Depolarisation Peaks. *J. Phys. D: Appl. Phys.* **1995**, *28*, 1478−1487.

(11) Correia, N. T.; Alvarez, C.; Moura Ramos, J. J.; Descamps, M. The $\beta-\alpha$ Branching in D-Sorbitol as Studied by Thermally Stimulated Depolarization Currents (TSDC). *J. Phys. Chem. B* **2001**, *105*, 5663−5669.

(12) Correia, N. T.; Moura Ramos, J. J.; Descamps, M.; Collins, G. Molecular Mobility and Fragility in Indomethacin: A Thermally Stimulated Depolarisation Currents Study. *Pharm. Res.* **2001**, *18*, 1767−1774.

(13) Correia, N. T.; Diogo, H. P.; Moura Ramos, J. J., unpublished results.

(14) Dierking, I. *Textures of Liquid Crystals*; Wiley: Weinheim, 2003.

(15) Pershan, P. S. *Structure of Liquid Crystal Phases*; World Scientific: River Edge, NJ, 1988.

(16) Guillon, D. Columnar Order in Thermotropic Mesophases. In *Structure and Bonding*; Springer−Verlag: Berlin, 1999; Vol. 95, pp 41−82.

(17) Levelut, A M.; Hardouin, F.; Gasparoux, H.; Destrade, C.; Tinh, N. H. *J. Phys.* **1981**, *42*, 147−152.

(18) All calculations were performed using the GAUSSIAN 98 (G98W) and HyperChem5.1 programs.